Available online at www.sciencedirect.com

ScienceDirect

Procedia Structural Integrity 38 (2022) 283–291

Structural Integrity Procedia

www.elsevier.com/locate/procedia

FATIGUE DESIGN 2021, 9th Edition of the International Conference on Fatigue Design

Experimental study of a CoCrMo alloy treated by SMAT under rotating bending fatigue

L. BRASILEIRO[a], Z. SUN[a], C. MABRU[b], R. CHIERAGATTI[b], G. PROUST[c,d], D. RETRAINT[a]*

a- LASMIS, Université de Technologie de Troyes (UTT), Troyes 10000, France
b- ICA, Université de Toulouse, ISAE-SUPAERO, MINES ALBI, UPS, INSA, CNRS, Toulouse 31055, France
c-School of Civil Engineering, The University of Sydney, NSW 2006, Sydney, Australia.
d-Sydney Manufacturing Hub, The University of Sydney, NSW 2006, Australia

Abstract

The main objective of this work is to understand the fundamental damage mechanisms involved in a SMAT treated CoCrMo alloy subjected to fatigue under rotating bending loads. For this purpose, different load amplitudes in rotating bending are imposed on cylindrical specimens, in as-machined and SMAT states. Different material characterizations are performed in order to determine which features play an important role in fatigue life of the studied alloy. Such characterizations are done via digital microscopy, electron backscatter diffraction (EBSD), roughness measurements and microhardness tests. The fatigue results presented in the form of S-N diagram show that SMAT with a moderate intensity (SMAT-2) can enhance the fatigue performance of the CoCrMo alloy, whereas SMAT with a higher intensity (SMAT-3) seems to deteriorate it. This fatigue life decrease is probably due to surface micro-cracks generated by an over-peening phenomenon.

Keywords: SMAT, CoCrMo, rotating bending fatigue, microhardness, surface integrity

* Corresponding author. Tel.: +33-3-25-71-56-68
E-mail address: delphine.retraint@utt.fr

10.1016/j.prostr.2022.03.029

1. Introduction

The safety of mechanical parts used in several sectors of the industry is of great importance. Critical component parts are present in a diverse spectrum of the engineering sector, from engines, transportation infrastructure and vehicles, to bioengineering applications such as for human prosthesis. These components commonly undergo cyclic loads and vibrations while in use. Such cyclic loads can generate fatigue damage, which in general initiates at the surface of the component, causing local stress concentration. Much effort has been made to enhance the mechanical strength of parts and to gain a better understanding of the fatigue properties of materials. Each applied treatment is specific to every material according to their use and mechanical features.

To strengthen materials and therefore improve their mechanical properties, some of the most widely used techniques are surface mechanical treatments, such as shot peening (Wu D., 2018; Yoon S. J., 2012; Torres M. A. S., 2002; Liu Z. G., 2017; Benedetti M., 2009), fine particle bombarding (Morita T., 2012), rolling treatments (Bormann T., 2020; Mori M., 2016; Wang H., 2018) or conventional hot-compression (Yamanaka K., 2009). Among them, Surface Mechanical Attrition Treatment (SMAT) has great potential for strengthening mechanical components subjected to cyclic loads. This treatment is based on multidirectional impacts of spherical balls set in motion using an ultrasonic generator (Li D., 2009; Gallitelli D., 2014; Wu Y., 2019; Roland T., 2006; Nkonta D. V. T., 2017; Gao T., 2020). SMAT is able to generate a nanocrystalline layer on the extreme surface of the treated part as well as a transition layer characterized by a grain size and a hardness gradient below the treated surface. In addition, high compressive residual stresses can be generated especially in the near-surface region where the plastic deformation is highly activated. Studies presented in the literature show that SMAT is able to significantly improve the properties of various materials and more particularly their fatigue resistance (Li D., 2009, Gallitelli D., 2014, Roland T., 2006; Gao T., 2020). However, some studies showed some limitations to the treatment effectiveness, mainly due to its intensity. Many treatment parameters, such as the ball material, the time and amplitude of the treatment may lead to undesired effects like surface cracks that could induce earlier failure (Gao T., 2020; Zhou J., 2017; Maurel P., 2020).

In this paper, the fatigue properties of a CoCrMo alloy treated by SMAT are studied through rotating bending tests with several stress amplitudes mainly in the high cycle fatigue regime (HCF). First, the material characteristics and the experimental procedures are presented. The surface roughness and morphology, the hardness variations produced by SMAT and the fatigue test results are then presented. These results highlight the effects of two different SMAT processes on the fatigue properties of the studied alloy, when compared to the as-machined condition. The experimental results are then analyzed to understand why one SMAT condition is more suitable than another to enhance the fatigue properties of the studied Co-based alloy.

2. Materials and Experimental Procedures

2.1 Material

A low carbon warm-worked CoCrMo alloy was investigated in this study. CoCrMo is a hard alloy with a high wear and corrosion resistance. It is used in different fields of the industry, from the aerospace sector to produce blades of aircraft engines, gas turbines and nozzle of diesel engines, to bioprosthesis used in humans (Yamanaka K., 2009, Nkonta D. V. T., 2017; Demangel C., 2014). The studied CoCrMo alloy has an equiaxed grained microstructure (Fig. 1) with an average grain size of 10 µm and is composed of a dominant phase FCC-ɣ with an HCP-ε phase. In this work, the material was received in the form of a cylindrical bar with a diameter of 12 mm. Its nominal chemical composition is shown in Table 1. The mechanical properties of this alloy according to the manufacturer are: yield strength of 1040 MPa and ultimate tensile strength of 1430 MPa. Rotating bending fatigue specimens were machined, and the shape and dimensions of the fatigue specimens are shown in Fig. 2.

Table 1. Chemical composition of CoCrMo (in wt%).

Co	Cr	Mo	Mn	Si	Fe	N	C	W	Cu	P	S	Nb	Al	Ti	B
65.12	27.27	5.44	0.7	0.67	0.42	0.17	0.03	0.03	LT.03	0.003	0.002	0.012	0.005	0.05	0.002

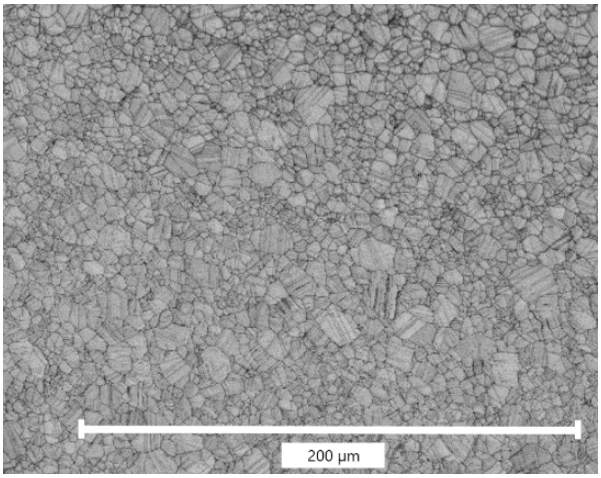

Fig. 1. Microstructure observation (band contrast map obtained by EBSD) of the studied CoCrMo alloy in the untreated condition.

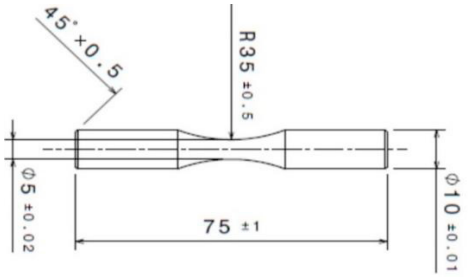

Fig. 2. The rotating bending fatigue sample geometry and dimensions (in mm).

2.2 Experimental details

In order to understand the effects of SMAT on the fatigue properties of the CoCrMo alloy, three conditions were considered for this work: as-machined (untreated), SMAT-2 (SMAT with 2 mm 100Cr6 steel balls) and SMAT-3 (SMAT with 3 mm 100Cr6 steel balls). Both SMAT treatments were performed using a generator power of 52% and a coverage of 1500%. The fatigue tests were conducted using a sinusoidal load with a frequency of 70 Hz and a load ratio R = -1, at room temperature. Each fatigue test was stopped either when the specimen broke or when the cycle number reached a value of 10^7 cycles. The method chosen for the fatigue tests is the median S-N test method, as described by the JSME S 002, one of the most widely used by researchers for S-N curve and fatigue life determination. At least 14 samples are required, 6 of which are used to find the fatigue limit according to the staircase method (Lee Y. L., 2005).

2.3 Testing

Surface morphology and work hardened layer were evaluated for the three studied conditions. Surface roughness was measured by a 3D optical profilometer. The Gaussian filter was 0.8 mm for Rt and Rsm and the profile length ranged from 4.5 mm to 6.5 mm. The measurements were made on each sample at 5 different locations in the centre region of the specimen.

The microhardness was evaluated using a Vickers indenter. The measurements were carried out using a load of 25gf applied for 5s. They were performed on cross sections of the three groups of specimens at different depths from the surface until they approached the hardness of the core material. It was thus possible to estimate the thickness of

the work hardened layer generated by the two SMAT treatments on the CoCrMo alloy. Seven measurements were conducted at each depth and then averaged, in order to consider the material's heterogeneity and measurement errors. Before carrying out the hardness measurements, the samples were first cut transversely, embedded in resin and then mirror polished, using SiC papers up to 1200 grade and then polished with diamond paste down to 1μm.

The microstructure of the alloy was characterized using electron backscatter diffraction (EBSD), after the specimen was polished using a 60 nm colloidal solution as the last step, in a scanning electron microscope (SEM, Zeiss Ultra) equipped with an Oxford Instruments' Nordlys-nano detector.

3. Experimental Results

3.1 Surface roughness and morphology

When evaluating the effects of surface mechanical treatments, it is important to consider the surface properties, as they may induce local surface stress concentration and thus reduce the fatigue performance (Zhou J., 2017; Maurel P., 2020). First, the surface topography was observed using a digital microscope. It is possible to see differences on the surface morphologies of all groups, as shown in Fig. 3. Figs. 3a, b and c present the surface of as-machined, SMAT-2 and SMAT-3 specimens, respectively. The machining grooves are visible along the specimen surface in Fig. 3a. The other conditions exhibit different features. Knowing that the ball size used for SMAT-3 is bigger (3 mm) compared to SMAT-2, deeper and wider imprints can be seen, while several micro-cracks also seem to be present (yellow arrows in Fig. 3e). Due to the higher kinetic energy involved in SMAT-3, and the same coverage as SMAT-2, it could be considered that there is an over-peening phenomenon generated by SMAT-3.

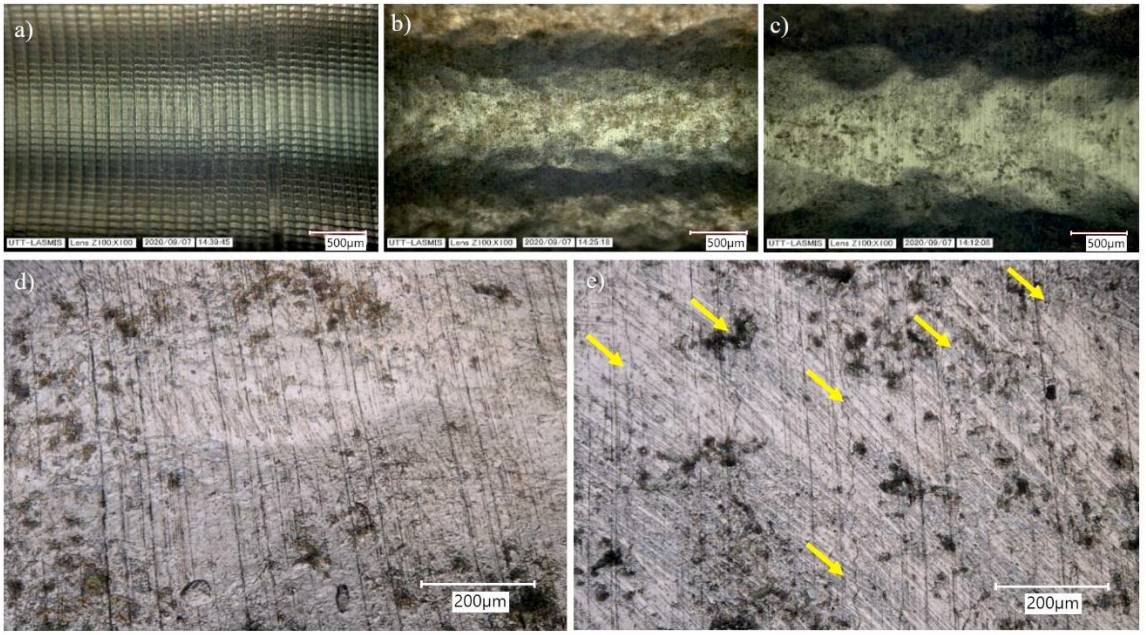

Fig. 3. Digital microscope observation of the surface topography after different processes: (a) as-machined (untreated) condition, (b) SMAT-2, (c) SMAT-3, (d) magnified view of SMAT-2, and (e) magnified view of SMAT-3. The yellow arrows indicate surface micro-cracks.

The surface profiles of the three types of samples are shown in Fig. 4. It is possible to notice that the profile for the as-machined specimen (Fig. 4a) presents greater peaks and valleys, compared to the treated SMAT-3 and SMAT-2 specimens (Figs. 4b and c respectively). This corresponds to the traces generated by the machining process.

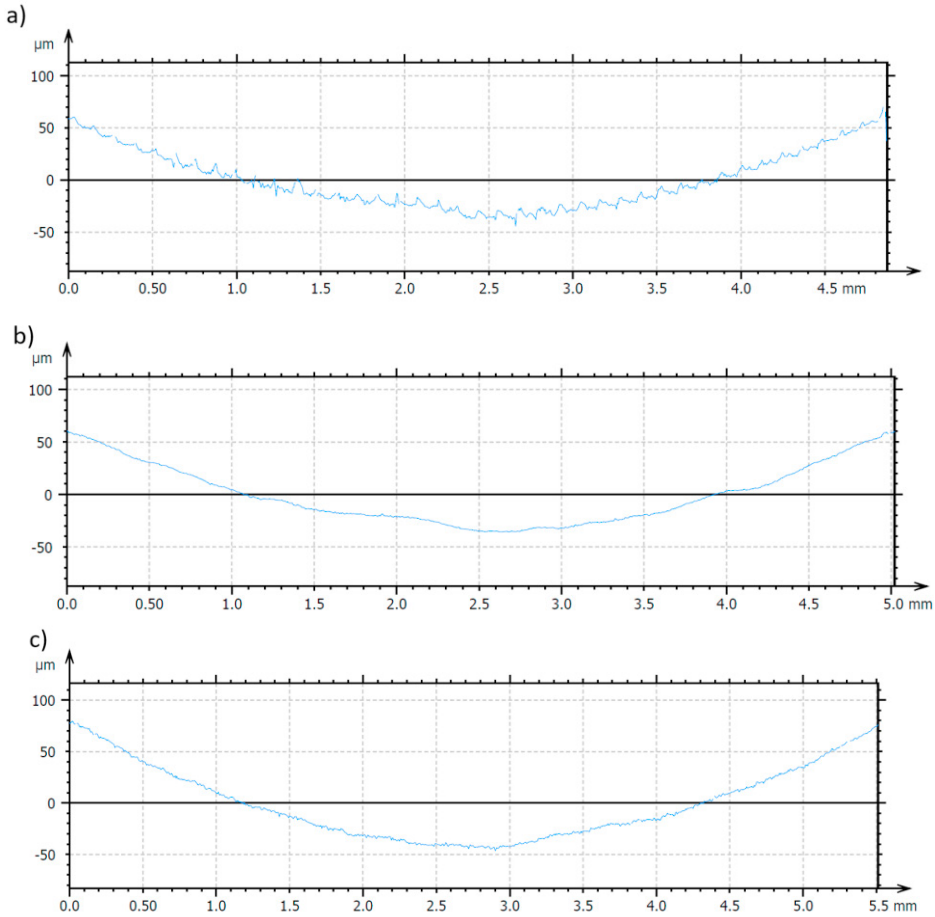

Fig. 4. Surface profiles measured along the axial direction of samples in the conditions: (a) as-machined, (b) SMAT-3, and (c) SMAT-2.

A drastic reduction in roughness can be observed after both SMAT treatments. It can be explained by the bombardment of high kinetic energy balls inducing local plastic deformation, denting the peaks and valleys of the machining grooves that can no longer be detected (Figs. 4b and c). It is also important to consider the high coverage for both SMAT conditions (1500%), asserting that the whole fatigue tested zone is deeply impacted. In order to quantitatively characterize the surface state of the three groups of samples, the most preponderant surface roughness parameters were considered. A mean value of the different measurements is presented in Fig. 5.

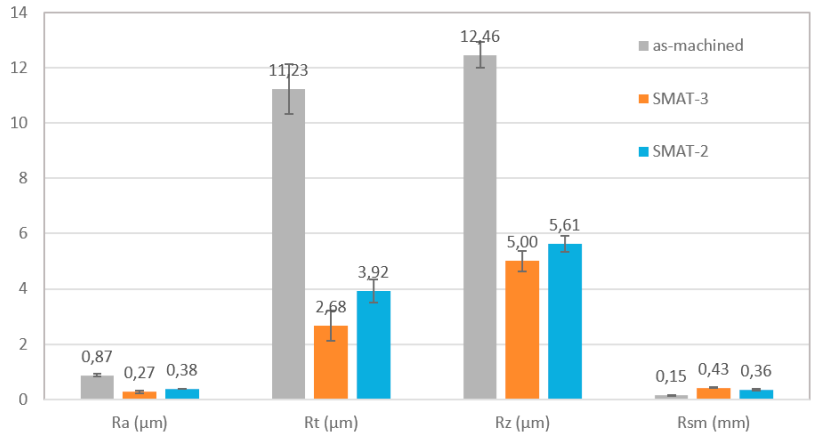

Fig. 5. Mean values of the average roughness (Ra), the total roughness (Rt), the maximum roughness (Rz) and the average width roughness (Rsm) under the three conditions studied.

An average of five measurements for each roughness parameter was taken into account. The roughness parameters are respectively the arithmetic mean roughness (Ra), the difference between the highest peak and the deepest valley (Rt), the maximum roughness (Rz) and the mean peak width (Rs_m). The parameters Rt and Rs_m can be used to calculate the stress concentration caused by surface roughness: the narrower the peak width, and the higher the peaks and valleys, the more locally concentrated a stress can be (Gao T., 2020; Benedetti M., 2009). Some studies suggested an increase in most roughness parameters after SMAT for surface polished specimens (Gallitelli D., 2014; Wu Y., 2019; Roland T., 2006; Nkonta D. V. T., 2017; Gao T., 2020; Zhou J., 2017). This is not the case for this work since the untreated condition corresponds to the as-machined state, for which Ra, Rt and Rz are 2 to 4 times bigger than for the SMAT-2 and SMAT-3 cases. This creates a possibility of enhancing a material's mechanical properties without the need of polishing. The difference in the ball size for SMAT-2 and SMAT-3 does not seem to have a preponderant role in the average roughness parameters, since they present very similar values. However, such values do not fully highlight other surface features such as micro-cracks highlighted above, which are commonly observed on over-peened materials (Zhou J., 2017; Maurel P., 2020).

3.2 Microhardness

The aim of the microhardness tests is to highlight a work-hardened layer induced by SMAT. The in-depth microhardness profiles were evaluated on resin embedded cross-sectional samples. As expected, the microhardness in the near surface region of the samples processed by SMAT has increased, compared to the untreated samples. The microhardness results show that SMAT-3 induces a thicker top surface work-hardened layer. As for SMAT-2, it generates a higher near to surface hardness (Fig. 6). As mentioned by Gao et al. (Gao T., 2020), a special attention should be given to severely SMAT treated surfaces due to the presence of surface defects, which could create earlier crack nucleation. A comparison between the two SMAT treatments, taking into account the ball size and the treatment time, may show differences such as dimples and micro-cracks (Gao T., 2020; Zhou J., 2017).

Considering a slight increase in the first hardness measurements on as-machined samples due to machining, the maximum top surface hardness values go from 465 ± 25 $HV_{0.025}$ in the untreated case, to 600 ± 25 $HV_{0.025}$ for the SMAT-2 processed sample. An increase is observed at about 20 µm below the surface. It is important to notice that despite an unexpected higher maximum hardness value for SMAT-2, due to its less severe SMAT condition, it does not keep an average hardness as high as SMAT-3. For both conditions, the hardness gradually decreases to a value of about 480 $HV_{0.025}$ at a depth of around 600 µm from the treated surface.

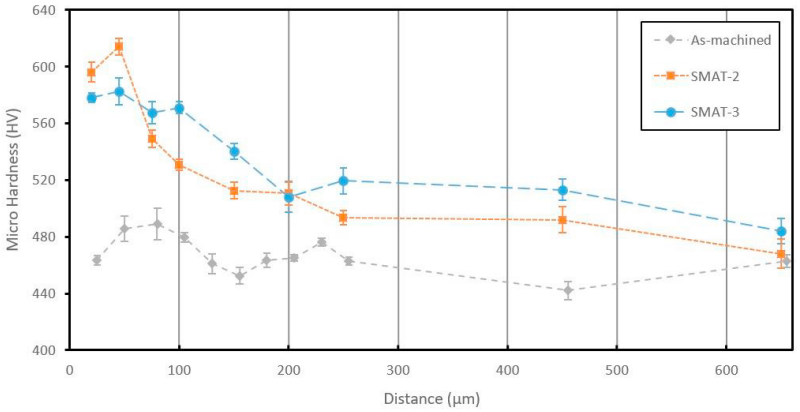

Fig. 6. Microhardness measurements of the CoCrMo alloy in the three conditions: as-machined, SMAT-2 and SMAT-3.

3.3 Fatigue Tests

The fatigue tests were performed according to the method proposed by the Japanese Society of Mechanical Engineers (JSME S 002, 1981). After the main parameters for the tests were designed, the fatigue lives for the specimens were evaluated at different load amplitudes. The purpose was to evidence which SMAT treatment (SMAT-2 or 3) is more effective for improving the fatigue strength under rotating bending fatigue. Replicate tests were carried out to ensure at least a reliability of 50% and the staircase method was used in order to determine the fatigue limit, based on the JSME S 002 standard. According to the first fatigue tests, the SMAT-2 condition seems to present overall better performance and less scattered results compared to the other conditions, as shown by the S-N diagram presented in Fig. 7. In addition, the fatigue lives of SMAT-3 vary and the stress dependency of fatigue life seems to be smaller. The line drawn at 10^7 cycles indicates that the material withstood the limit of cycles without failing.

So far, only the limited fatigue life zone has been investigated. In the future, by looking at the results of the replicate tests performed and in the unlimited fatigue life zone, it will be possible to estimate the corresponding fatigue limit for each condition by using the staircase method.

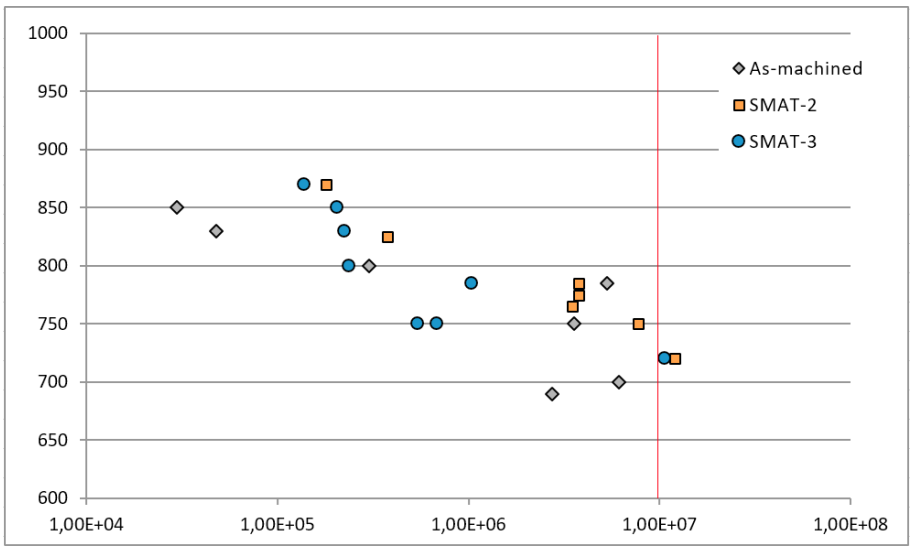

Fig. 7. First S-N curve including the three groups. The specimens are considered to have withstood the fatigue limit when they do not fail until 10^7 cycles (indicated by the vertical line).

4. Discussion and Analysis

SMAT can enhance the fatigue life of several materials subjected to cyclic loadings from low to high cycle regimes (Li D., 2009, Gallitelli D., 2014, Roland T., 2006; Gao T., 2020). It is important to take into account several factors to establish the ideal conditions for the treatment to a specific material including the size, dimensions and material of the balls used in the process as well as the sonotrode amplitude or the coverage value. Such conditions may induce beneficial effects such as work-hardening and compressive residual stresses into the surface and subsurface regions, where most cracks originate during fatigue tests, enhancing crack propagation resistance. Despite these positive effects generated by SMAT, this process may increase surface roughness, which can play an important role when it comes to local stress concentration (Kt). It may induce crack nucleation and depending on the material's notch sensitivity, the positive effects of SMAT may not be sufficient to stop crack propagation.

In this study, the surface roughness of the specimens in different conditions indicate a drastic reduction of this parameter compared to the as-machined condition. This can be considered as another positive feature of SMAT, since there would be no need of polishing to improve the surface properties. The arithmetic roughness (Ra) of the SMAT-3 and SMAT-2 treated specimens are 322% and 228% smaller than that of the as-machined, respectively. The decrease in the total roughness (Rt) values for both SMAT-treated specimens, an important parameter for Kt, was 419% and 286% compared to the as-machined specimens, respectively. The average stress concentration factors for the treated specimens were calculated according to Gao et al. (Gao T., 2020). These stress concentration factors were calculated for rough surfaces created by shot peening according to the following relation $\mathrm{Kt} = 1 + 2.1(\mathrm{Rt}/\mathrm{Rsm})$. The average Kt values are 1.013 for SMAT-3 and 1.022 for SMAT-2 respectively. These values indicate that the SMAT condition for SMAT-2 could lead to more severe surface damage in terms of surface roughness. However, as mentioned previously, severe conditions may introduce surface defects that are not detected by roughness profiles, such as micro-cracks (Gao T., 2020; Zhou J., 2017; Maurel P., 2020; Benedetti M., 2009).

It was noticed that for SMAT-3, the presence of micro cracks was rather evident, leading to a worse fatigue performance, as shown in Fig. 7. This suspicion is due to the fact that SMAT-3 presented a deeper work-hardened layer and lower surface roughness of all groups of specimens. Usually this combination leads to a better fatigue life which was not the case here. Residual stress profile measurements along the surface depth could confirm this hypothesis. It could also show if there was an introduction of compressive residual stress after machining for as-machined samples, as some of them had actually good fatigue resistance.

The results from the fatigue tests in the limited life regime seem to indicate that SMAT was effective for one of the two treatments. While SMAT-3 in several load amplitudes presented a lower fatigue life compared to the as-machined case, SMAT-2 specimens displayed overall better and less scattered results. These observations will be deeper statistically analyzed in a future study using the staircase method. Besides, fracture surface observations will be carried out in order to understand the mechanisms involved in the fatigue of this alloy with and without SMAT. These observations of crack initiation site and crack propagation area could reveal and explain a possible correlation between the presence of micro-cracks and the tendency observed in the S-N diagram.

5. Conclusions

This paper focused on evidencing experimentally the effects of SMAT on a CoCrMo alloy subjected to rotating bending fatigue. The experiments included the characterization of the surface integrity through roughness and surface morphology measurements, microhardness tests along the subsurface until the unaffected zone and fatigue tests. Conclusions of the effects of SMAT on fatigue life are summarized as follows:

- The fatigue life of the CoCrMo alloy can be enhanced by SMAT depending on the treatment conditions such as ball size, compared to the as-machined condition.
- For as-machined samples, one of the benefits of SMAT lies in reducing machining grooves to low roughness parameters, improving surface properties and avoiding local stress concentration, thus early crack nucleation.
- A severe SMAT condition can cause defects on the surface that may give rise to great local stress concentration, causing crack nucleation that can overwhelm the beneficial effects of the treatment.

As one of the parts of our future work, fracture surface observations especially on fatigue crack initiation site and early crack propagation area will be performed in order to explain the correlation between the surface micro-cracks and the tendency observed in the S-N diagram.

Acknowledgements

The authors acknowledge the financial support of the European Union (FEDER) and the Grand-Est Region through the SURFLEXFATIGUE project. The technical and scientific assistance of Sydney Microscopy & Microanalysis, the University of Sydney node of Microscopy Australia is greatly appreciated.

References

Benedetti M., Fontanari V., Scardi P., Ricardo C. L. A., Bandini M., 2009. Reverse bending fatigue of shot peened 7075-T651 aluminium alloy: The role of residual stress relaxation. International Journal of Fatigue 31, 1225–1236.

Bormann T., Phuong M. T., Gibmeier J., Sonntag R., Müller U., Kretzer J. P., 2020. Corrosion Behavior of Surface-Treated Metallic Implant Materials. Materials, 13, 2011.

Demangel C., Poznanski A., Steenhout V., Levesque A., Benhayoune H., Retraint D., 2014. Benefit of a Surface Nanocrystallization Treatment on Co28Cr6Mo Abrasive Wear Properties. Advanced Materials Research Vols. 966-967, 435-441.

Gallitelli D., Retraint D., Rouhaud E., 2014. Comparison between conventional shot peening (SP) and surface mechanical attrition treatment (SMAT) on a Titanium alloy. Advanced Materials Research Vol 996, pp 964-968.

Gao T., Sun Z., Xue H., Retraint D., 2020. Effect of surface mechanical attrition treatment on high cycle and very high cycle fatigue of a 7075-T6 aluminium alloy. International Journal of Fatigue 139, 105798.

Gao T., Sun Z., Xue H., Bayraktar E., Qin Z., Li B., Zhang H., 2020. Effect of Turning on the Surface Integrity and Fatigue Life of a TC11 Alloy in Very High Cycle Fatigue Regime. Metals, 10, 1507.

Lee Y. L., Pan J., Hathaway R., Barkey M., 2005. Fatigue Testing and Analysis: Theory and Practice, Chapter 4 Stress Based Fatigue Analysis and Design pp.183 - 178.

Li D., Chen H. N., Xu H., 2009. The effect of nanostructured surface layer on the fatigue behaviors of a carbon steel. Applied Surface Science 255, 3811–3816.

Liu Z. G., Wong T. I., Huang W., Sridhar N., Wang S. J., 2017. Effect of Surface Polishing Treatment on the Fatigue Performance of Shot-Peened Ti–6Al–4V Alloy. Acta Metall. Sin. (Engl. Lett.), 30(7), 630–640.

Maurel P., Weiss L., Grosdidier T., Bocher P., 2020. How does surface integrity of nanostructured surfaces induced by severe plastic deformation influence fatigue behaviors of Al alloys with enhanced precipitation?. International Journal of Fatigue 140, 105792.

Mori M., Yamanaka K., Chiba A., 2016. Cold-rolling behavior of biomedical Ni-free Co–Cr–Mo alloys: Role of strain-induced ε martensite and its intersecting phenomena. Journal of the mechanical behavior of biomedical Materials 55 201–214.

Morita T., Nakaguchi H., Noda S., Kagaya C., 2012. Effects of Fine Particle Bombarding on Surface Characteristics and Fatigue Strength of Commercial Pure Titanium - Materials Transactions, The Japan Institute of Metals.

Nkonta D. V. T., 2017. Caractérisation de l'effet de traitement de nanocristallisation superficielle (SMAT) sur un alliage CoCrMo. Université de Technologie de Troyes, France.

Torres M. A. S., Voorwald H. J. C., 2002. An evaluation of shot peening, residual stress and stress relaxation on the fatigue life of AISI 4340 steel. International Journal of Fatigue 24, 877–886.

Roland T., Retraint D., Lu K., Lu J., 2006. Fatigue life improvement through surface nanostructuring of stainless steel by means of surface mechanical attrition treatment. Scripta Materialia 54, 1949–1954.

Wang H., Yang X., Li H., Song G., Tang G., 2018. Enhanced fatigue performance and surface mechanical properties of AISI 304 stainless steel induced by electropulsing-assisted ultrasonic surface rolling process. J. Mater. Res., Vol. 33, No. 22.

Wu D., Yao C., Zhang D., 2018. Surface characterization and fatigue evaluation in GH4169 superalloy: Comparing results after finish turning; shot peening and surface polishing treatments. International Journal of Fatigue 113, 222–235.

Wu Y., Guelorget B., Sun Z., Déturche R., Retraint D., 2019. Characterization of gradient properties generated by SMAT for a biomedical grade 316L stainless steel. Materials Characterization 155, 109788.

Yamanaka K., Mori M., Kurosu S., Matsumoto H., Chiba A., 2009. Ultrafine Grain Refinement of Biomedical Co-29Cr-6Mo Alloy during Conventional Hot-Compression Deformation. Metallurgical and Materials Transactions A.

Yoon S. J, Park J. H., Choi. N. S., 2012. Fatigue life analysis of shot-peened bearing steel. Journal of Mechanical Science and Technology 26 (6), 1747-1752.

Zhou J., Sun Z., Kanouté P., Retraint D., 2017. Effect of surface mechanical attrition treatment on low cycle fatigue properties of an austenitic stainless steel. International Journal of Fatigue 103, 309–317.